Proceedings of the
Annual Stability Conference
Structural Stability Research Council
San Antonio, Texas, March 19-22, 2024

Analytical Equations for Critical Local Buckling Stress of Cold-Formed Steel Lipped Channel Sections with Centered Web Holes

Chu Ding[1], Robert S. Glauz[2], Benjamin W. Schafer[3]

Abstract

The objective of this research is to develop accurate analytical equations for cold-formed steel lipped channel sections with centered web holes. The proposed equations can be used as an alternative to computational methods (e.g., finite strip analysis) for accurately determining critical buckling loads or moments, which are inputs to the Direct Strength Method for member design. Analytical equations are developed separately for lipped channel sections without holes and sections with centered web holes. For each case, finite strip analyses are performed for over 1000 lipped channel sections with a wide range of geometric ratios. Equations in the form of polynomial ratios are fitted to the analysis results. The effect of hole length on critical local buckling stress is considered by proposing a length-dependent correction factor curve fitted to analysis results. Proposed analytical equations are found to have excellent prediction accuracy and greatly exceed the performance of the current isolated element methods in the AISI S100 Appendix 2. It is believed that the proposed equations will effectively reduce the barrier to Direct Strength Method and simplify the steps to integrate the method into typical cold-formed steel design workflows.

1. Introduction

Lipped channel sections are widely used in the cold-formed steel (CFS) framing industry (Fig. 1). The design of lipped channel CFS members includes checking various buckling limit states, one of which is local buckling. In the North American cold-formed steel design specification AISI S100 (2020), the default design method to check the local buckling limit state is the Direct Strength Method (DSM). To use DSM for local bucking check, engineers are required to first determine the elastic critical local buckling stress ($F_{cr\ell}$) of the cross-section.

[1] Adjunct Assistant Research Scientist, Johns Hopkins University, cding6@alumni.jh.edu
[2] Owner, RSG Software, Inc., glauz@rsgsoftware.com
[3] Professor, Johns Hopkins University, schafer@jhu.edu

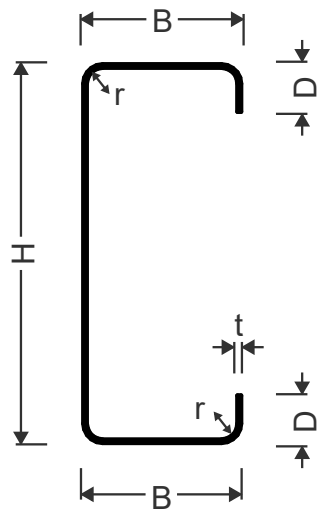

Figure 1: Typical lipped channel section annotated with out-to-out dimensions *H*, *B*, *D*, inside corner radius *r*, and uncoated thickness *t*.

In the current AISI specification, there are two methods for determining elastic critical local buckling stress: the numerical method and the element method. Both methods are detailed in Appendix 2. The numerical method refers to running finite strip analysis or shell finite element analysis to determine section critical local buckling stress. The element methods refer to using analytical equations to determine single plate local buckling stress and aggregating the results into section-level critical local buckling stresses. Element methods in similar formats are also provided in Australian and New Zealand standard AS/NZS 4600 (2018) and Eurocode EN-1993-1-5 (2006). Both numerical and element methods have disadvantages in practice. Though capable of generating accurate results, the numerical method has a high barrier to entry for practicing engineers because it requires software and is not easily integrated with spreadsheet based workflows. The element method also has limitations. First, the method is less accurate because it ignores interactions between connecting plates and provides limited consideration of hole sizes for sections with holes. Second, the method can be complicated to use for bending cases because element buckling stresses need to be converted to the same locations on the section and compared so that the controlling bucking stress can be selected. Due to these disadvantages, it is desirable to develop a new method that is both accurate and easy to use.

2. Buckling stress equations developed from finite strip analysis

Finite strip analysis is capable of generating critical buckling stress and is relatively inexpensive to run; because of these features, finite strip analysis has been used to develop analytical equations for buckling stresses in various studies. Seif and Schafer (2010) and Gardner et al. (2019) proposed analytical equations for critical local buckling stresses for a variety of hot-rolled structural steel shapes, which led to improved accuracy over the equations used in AISC specifications and Eurocode. Efforts have been made for cold-formed steel as well: de Miranda Batista (2010) proposed equations for buckling coefficients of several CFS sections under pure compression and major axis bending, and those equations were adopted in the Brazilian CFS design code. In a recent study, Ahdab et al. (2022) proposed a series of local buckling stress equations for a variety of loading conditions. Despite the efforts in recent years, there have been only limited studies

focusing on developing equations for sections with holes. As holes are ubiquitous in the cold-formed steel framing industry, accurate and easy-to-use analytical equations for sections with holes hold high practical significance for practicing engineers. This study is aimed at leveraging finite strip analysis to develop a set of accurate and easy-to-use analytical equations for calculating elastic critical local buckling stresses.

3. Existing methods for calculating critical local buckling stress

Analytical equations are provided in the AISI S100 Appendix 2 to calculate elastic critical local buckling stresses of individual elements of a cross-section. To arrive at the section-level local buckling stress needed for using DSM, engineers need to follow a procedure involving two steps. First, the buckling stresses of individual elements of the cross-section are calculated per equations provided in Appendix 2. Second, the section-level local buckling stress is selected among those element-level stresses based on whichever leads to the lowest buckling load or moment. In AISI S100 Appendix 2, the equations for element-level local buckling stress follow the format of classical plate buckling theory as expressed by Eq. 1.

$$F_{cr\ell} = k\frac{\pi^2 E}{12(1-\mu^2)}\left(\frac{t}{w}\right)^2 \tag{1}$$

where k is the plate buckling coefficient, E is Young's modulus, μ is Poisson's ratio, t is plate thickness, and w is plate flat width.

The plate buckling coefficient defined in Eq. 1 is not only dependent on boundary conditions, but also on stress gradients. The plate buckling coefficients under various conditions are summarized below.

For stiffened elements under uniform compression k = 4. For unstiffened element under uniform compression, k = 0.43.

For stiffened elements under stress gradient ψ:
(1) For elements with both compression and tension stress

$$k = 4 + 2(1+\psi)^3 + 2(1+\psi) \tag{2}$$

where $\psi = |f_2/f_1|$, f_1 is the compression stress and f_2 is the tension stress
(2) For elements with compression stress only

$$k = 4 + 2(1-\psi)^3 + 2(1-\psi) \tag{3}$$

where $\psi = |f_2/f_1|$, $f_2 \leq f_1$

For unstiffened elements under stress gradient ψ:
(1) For elements with compression only and stress decreases toward the unsupported edge

$$k = 0.578/(\psi + 0.34) \tag{4}$$

where $\psi = |f_2/f_1|$, $f_2 \leq f_1$
(2) For elements with compression only and stress increases toward the unsupported edge

$$k = 0.57 - 0.21\psi + 0.07\psi^2 \tag{5}$$

where $\psi = |f_2/f_1|$, $f_2 \leq f_1$
(3) For elements with supported edge in tension and unsupported edge in compression

$$k = 0.57 + 0.21\psi + 0.07\psi^2 \quad (6)$$

where $\psi = |f_2/f_1|$, f_1 is the compression stress and f_2 is the tension stress

(4) For elements with supported edge in compression and unsupported edge in tension

$$k = 1.70 + 5\psi + 17.1\psi^2 \quad (7)$$

where $\psi = |f_2/f_1|$, f_1 is the compression stress and f_2 is the tension stress

4. Finite strip analysis study

A finite strip analysis study is conducted to generate data for developing analytical equations. In the study, finite strip analyses are performed on 1228 lipped channel cross sections including both commercial SFIA cross-sections and non-commercial sections. The non-commercial sections are created within a set of geometric constraints: 0.05 < B/H <0.75, 0.1 < D/B < 0.4, B/t > 8, and D/t > 4. For each cross-section, analysis is performed for both a gross section model without a hole and a net section model with a centered web hole (Fig. 2). In the net section model, the web portion is modeled as two unstiffened elements. Standard hole sizes are used in the models, which are referenced from AISI S240 (2020) and SFIA (2018). Specifically, the hole width is 0.75 in. (19 mm) if a section is shallower than 2.5 in. (63.5 mm). If a section depth is equal to or deeper than 2.5 in. (63.5 mm), the hole width is 1.5 in. (38 mm). The hole length is 4 in. (102 mm) regardless of section depth. Additionally, analysis is performed separately for four different loading conditions: pure compression, major-axis bending, minor-axis bending with lip in compression, and minor-axis bending with lip in tension. The critical local buckling mode is determined using a two-step method proposed by Li and Schafer (2010).

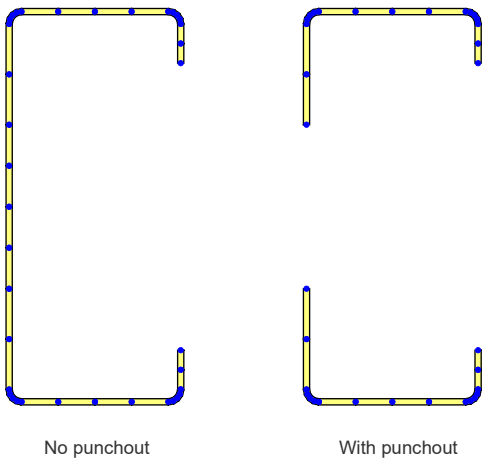

Figure 2: Finite strip models of lipped channel sections without hole (left) and with a centered web hole (right)

For sections with holes, determining the elastic critical local buckling stresses requires considering the influence of hole length. An approximate approach proposed by Moen and Schafer (2009) is used in this study. Specifically, for each finite strip analysis, the critical local buckling half-wavelength $L_{cr\ell}$ is compared against the hole length L_h. If $L_{cr\ell} \leq L_h$, the local buckling stress corresponding to $L_{cr\ell}$ is selected as the section critical local buckling stress $F_{cr\ell}$. If $L_{cr\ell} > L_h$, the local buckling stress corresponding to L_h is selected instead as the section $F_{cr\ell}$. This approach

avoids the need for expensive finite element analysis using shell elements and has been included in the Commentary of Appendix 2 in the AISI S100.

5. Develop analytical equations from finite strip analysis

The target analytical equations are formulated as classical plate buckling equations with custom-defined plate buckling coefficients as expressed in Eq. 8. Analytical equations are developed for the plate buckling coefficients, which depend on a variety of parameters including type of loading, cross-section geometric ratio, stress gradient, and hole dimension. The main focus is developing equations for predicting plate buckling coefficients given cross-sections and types of loading. Local buckling stresses determined from finite strip analysis are converted to corresponding plate buckling coefficients and serve as data for curve-fitting. It is worth noting that centerline dimensions (see Fig. 3) are used in all proposed analytical equations.

$$F_{cr\ell} = k_w \frac{\pi^2 E}{12(1-\mu^2)} \left(\frac{t}{w}\right)^2 \tag{8}$$

where $F_{cr\ell}$ is elastic critical local buckling stress, and k_w is plate buckling coefficient

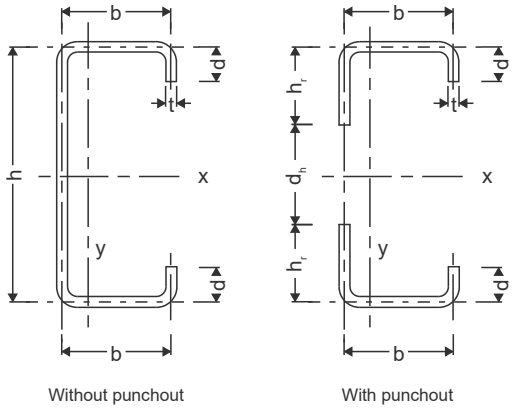

Figure 3: Centerline dimensions of lipped channel sections

2.1 Sections without holes

Using the finite strip analysis data, analytical equations are proposed for lipped channel sections without holes under different loading conditions. The general format of the proposed equations is a classical plate buckling equation with the plate buckling coefficient defined by additional equations. The choice of plate buckling coefficient varies among loading conditions. For pure compression and minor axis bending with lip in tension, the web plate buckling coefficient is used. For minor axis bending with lip in compression, the flange plate buckling coefficient is used. For the major axis bending, the plate buckling coefficient is the web coefficient or flange coefficient dependent on the geometric ratio h/b. The empirical equations of the plate buckling coefficients are expressed as ratios of polynomials. The parameters of polynomials include geometric ratios (e.g., web depth over flange width) and stress gradients. It is worth noting that applicable limits are also provided for each proposed equation. The limits are based on the coverage of the finite strip analysis data in various parameter domains.

The proposed equations are summarized as follows:

For pure compression

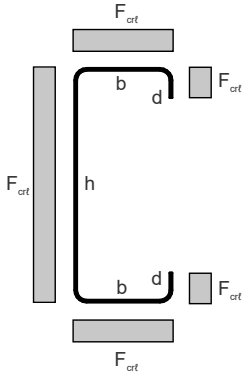

$$F_{cr\ell} = k_h \frac{\pi^2 E}{12(1-\mu^2)} \left(\frac{t}{h}\right)^2 \tag{9}$$

$$k_h = 4 + \frac{1.2\eta_h}{1 + 0.22\eta_h + 0.05\eta_h^2} \tag{10}$$

where

$\eta_h = h/b$

Applicable for $1.2 \leq \eta_h \leq 22$ and $r/t \geq 1.5$

For major axis bending

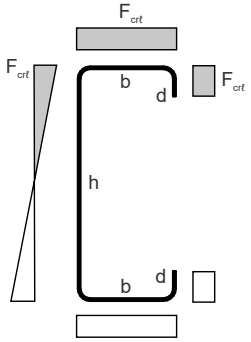

When $1.2 \leq \eta_h < 2.30$

$$F_{cr\ell} = k_b \frac{\pi^2 E}{12(1-\mu^2)} \left(\frac{t}{b}\right)^2 \tag{11}$$

When $\eta_h \geq 2.30$

$$F_{cr\ell} = k_h \frac{\pi^2 E}{12(1-\mu^2)} \left(\frac{t}{h}\right)^2 \tag{12}$$

$$k_b = \frac{4.93 - 3.15\eta_h + 0.53\eta_h^2}{1 - 0.64\eta_h + 0.11\eta_h^2} \tag{13}$$

$$k_h = \frac{-4.3\eta_h + 6.44\eta_h^2}{1 - 0.54\eta_h + 0.24\eta_h^2} \tag{14}$$

where

$\eta_h = h/b$

Applicable for $1.2 \leq \eta_h \leq 22$ and $r/t \geq 1.5$

For minor axis bending with lip in compression

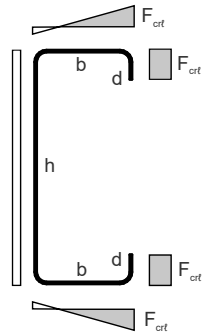

$$F_{cr\ell} = k_b \frac{\pi^2 E}{12(1-\mu^2)} \left(\frac{t}{b}\right)^2 \tag{15}$$

$$k_b = k_{b1} + k_{b2} \tag{16}$$

$$k_{b1} = 4 + \frac{0.8 - 0.758\eta_b + 0.234\eta_b^2}{1 - 0.533\eta_b + 0.09\eta_b^2} \tag{17}$$

$$k_{b2} = \begin{cases} 0 & \eta_b \le 2.75 \\ (4\eta_b - 11)\psi & 2.75 < \eta_b \le 6 \\ 13\psi & \eta_b > 6 \end{cases} \tag{18}$$

where
$\eta_b = b/d$
$\psi = |f_2/f_1|$
f_1 = Maximum compression stress in flange element
f_2 = Maximum tension stress in flange element

Applicable for $2.5 \le \eta_b \le 11.1$, $0.07 \le \psi \le 0.77, d/t \ge 4.4$ and $r/t \ge 1.5$

For minor axis bending with lip in tension

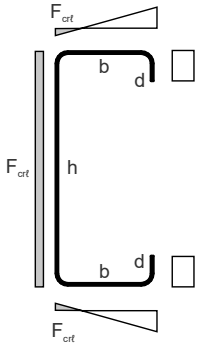

$$F_{cr\ell} = k_h \frac{\pi^2 E}{12(1-\mu^2)} \left(\frac{t}{h}\right)^2 \tag{19}$$

$$k_h = 4 + \frac{1.36 - 0.014\eta_h}{1 - 0.12\eta_h + 0.012\eta_h^2} \tag{20}$$

where
$\eta_h = h/b$

Appliable for $1.2 \le \eta_h \le 22$ and $r/t \ge 1.5$

The proposed equations are found to have excellent accuracy and consistency. As shown in Fig. 4, the proposed equations match well with analysis data for all loading conditions considered in this study. Additionally, calculations are performed to determine the finite strip to predicted ratios, which are the ratios of local buckling stresses determined from finite strip analysis (F_{FSM}) over the counterparts predicted by the proposed equations (F_{pred}). The mean finite strip to predicted ratios range from 0.99 to 1.02 and the corresponding COV range from 0.01 to 0.05 (see Table 1).

The proposed equations show clear improvements over the existing AISI analytical equations. In Fig. 5, comparison is made between the distributions of F_{FSM} to F_{pred} ratios under proposed equations and those under existing AISI equations. The ratios under the existing AISI equations are generally conservative and spread across wide spectrums. In comparison, the ratios under the proposed equations are generally within a range between 0.95 and 1.05.

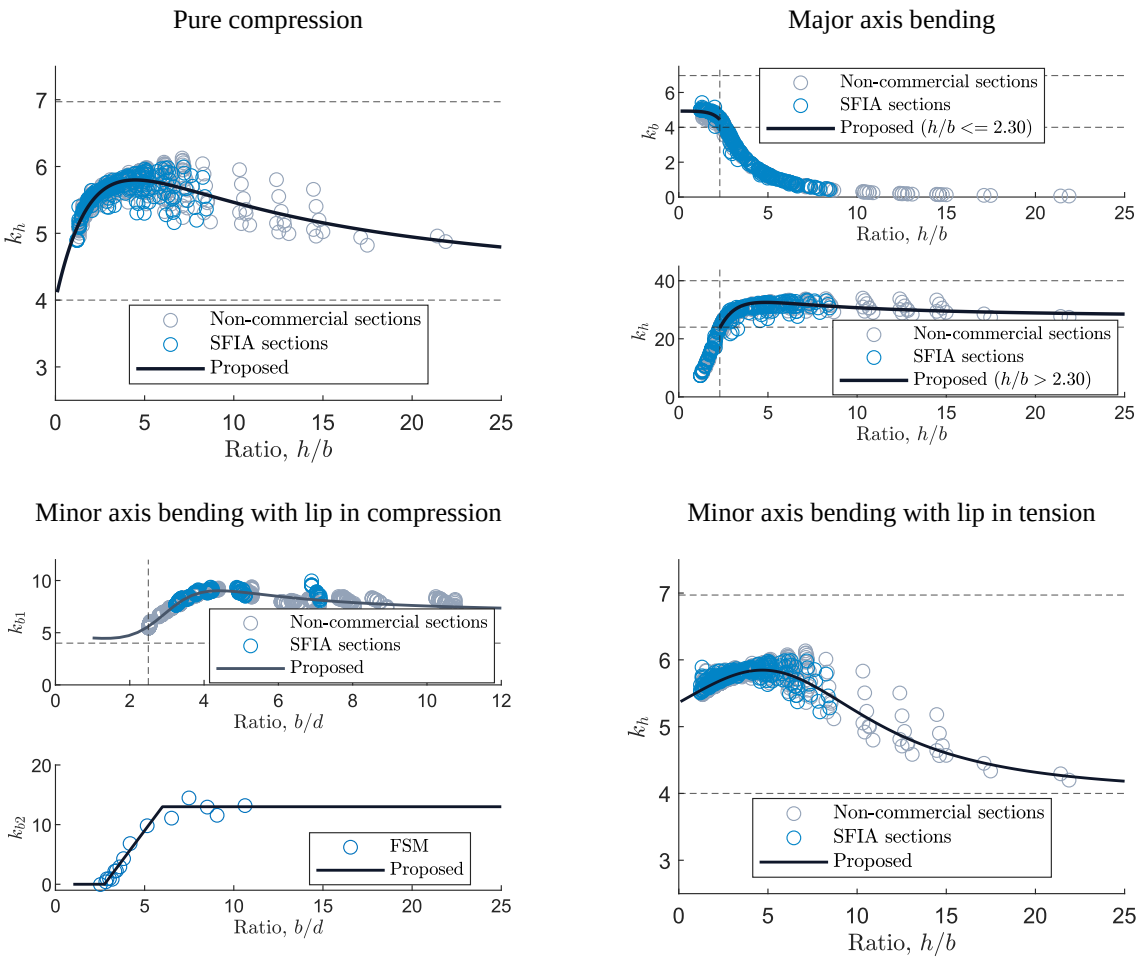

Figure 4: Proposed equations for sections without holes compared to finite strip analysis data

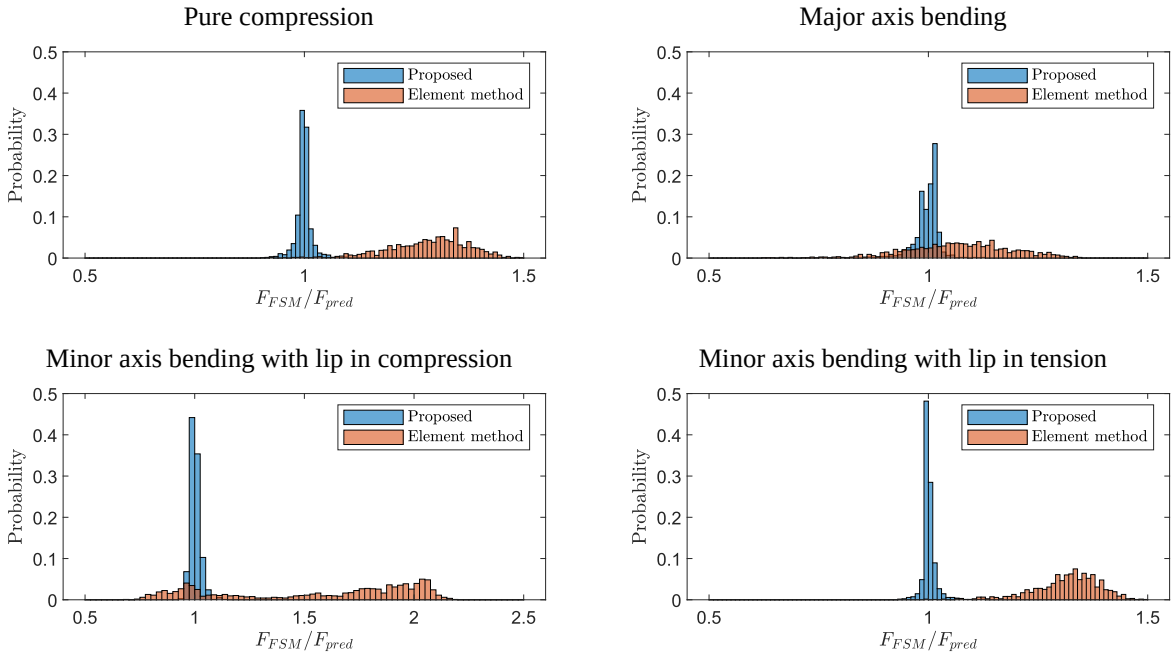

Figure 5: Histogram of the accuracy of the proposed equations for sections without holes

Table 1: Statistical summary of proposed equations for sections without holes

	SFIA (n=244)		Non-commercial (n=984)	
Loading case	Mean	COV	Mean	COV
Pure compression	1.00	0.02	1.00	0.02
Major axis bending	0.99	0.05	1.00	0.02
Minor axis bending with lip in compression	1.02	0.02	1.00	0.02
Minor axis bending with lip in tension	1.00	0.02	1.00	0.01

5.2 Sections with centered web holes

Using the finite strip analysis data, analytical equations are proposed for lipped channel sections with centered web holes. Similar to the proposed equations for sections without holes, the equations herein are formulated as classical plate buckling equations with newly defined plate buckling coefficients. Different from sections without holes, the plate buckling coefficients for sections with holes are expressed as a product of two parameters k_{w0} and C_{hs}. The parameter k_{w0} corresponds to the plate local coefficient responsible for the local buckling stress without considering the limit of hole length. Depending on the type of loading, k_{w0} can be expressed as either k_{hr0} (unstiffened web) or k_{b0} (flange). The parameter C_{hs} is the hole length modification factor corresponding to standard web hole length. For each loading type, analytical equations are proposed for k_{w0} and C_{hs}.

For the case of minor-axis bending with lip in compression, the same equation proposed for sections without holes can be re-used for sections with centered web holes, because the cross-section's web is under tension.

The proposed equations are summarized as follows:

For pure compression

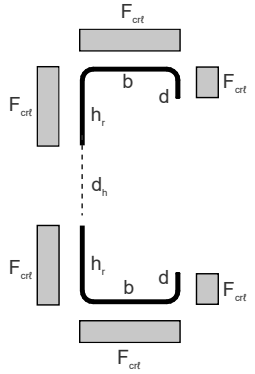

$$F_{cr\ell} = k_{hr}\frac{\pi^2 E}{12(1-\mu^2)}\left(\frac{t}{h_r}\right)^2 \tag{21}$$

$$\mathrm{k_{hr}} = C_{hs}k_{hr0} \tag{22}$$

$$k_{hr0} = \frac{1.02}{1+0.04\eta_{hr}^3} \geq 0.43 \tag{23}$$

$$C_{hs} = \frac{0.14\rho_d + 0.15}{\rho_d - 0.05} \geq 1 \tag{24}$$

where
$\eta_{hr} = b/h_r$
$\rho_d = d_h/h$

Applicable to $\eta_{hr} \leq 3, 0.09 \leq d_h/h \leq 0.52$, and $r/t \geq 1.5$

For major axis bending

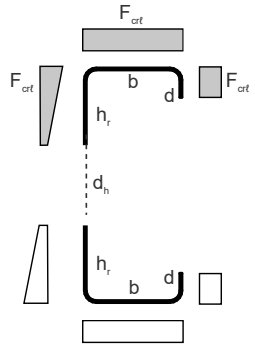

$$F_{cr\ell} = k_b\frac{\pi^2 E}{12(1-\mu^2)}\left(\frac{t}{b}\right)^2 \tag{25}$$

$$k_b = C_{hs}k_{b0} \tag{26}$$

When $\eta_{hrp} < 0.30$

$$k_{b0} = \frac{2.952\eta_{hrp}^2}{1-2.142\eta_{hrp}^2} \tag{27}$$

When $\eta_{hrp} \geq 0.30$

$$k_{b0} = \frac{0.152 + 6.974\eta_{hrp}^3}{1+1.277\eta_{hrp}^3} \tag{28}$$

$$C_{hs} = \frac{0.502\rho_d^* + 0.093}{\rho_d^* - 0.055} \geq 1 \tag{29}$$

where
$\eta_{hrp} = (b/h_r)(1-0.75\psi)$,
$\psi = |f_2/f_1|$
f_1 = Maximum compression stress in the unstiffened web element
f_2 = Minimum compression stress in the unstiffened web element

$$\rho_d^* = d_h/(h - 0.3b - 0.3d)$$

Applicable for $\eta_{hrp} \leq 2$, $0.09 \leq \psi \leq 0.52$, $0.09 \leq d_h/h \leq 0.52$, and $r/t \geq 1.5$

For minor axis bending with lip in compression, the same equations developed for sections without holes also apply herein.

For minor axis bending with lip in tension

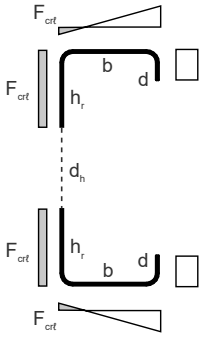

$$F_{cr\ell} = k_{hr}\frac{\pi^2 E}{12(1-\mu^2)}\left(\frac{t}{h_r}\right)^2 \quad (30)$$

$$k_{hr} = C_{hs}k_{hr0} \quad (31)$$

When $\eta_{hr} < 0.4$

$$k_{hr0} = \frac{1.15\eta_{hr}}{0.05 + \eta_{hr}} \geq 0.43 \quad (32)$$

When $\eta_{hr} \geq 0.4$

$$k_{hr0} = 1.04 - 0.04\eta_{hr} \geq 0.43 \quad (33)$$

$$C_{hs} = \frac{0.11\rho_d + 0.15}{\rho_d - 0.05} \geq 1 \quad (34)$$

where
$\eta_{hr} = b/h_r$
$\rho_d = d_h/h$

Applicable for $\eta_{hr} \leq 3$, $0.09 \leq d_h/h \leq 0.52$, and $r/t \geq 1.5$

The proposed equations are found to have good accuracy and low variation. According to Table 2, the mean F_{FSM} to F_{pred} ratios for all four loading types are between 0.99 and 1.01 and the COV falls within the range of [0.01, 0.06]. The proposed equations for k_{w0} and C_{hs} match well with the finite strip analysis data as shown in Fig. 6, where the proposed equations are compared with the data. As evidenced by Fig. 7, the performance of the proposed equations greatly exceeds that of the existing AISI equations for sections with holes. The existing AISI equations show inconsistent accuracy and high variations in performance across the dataset. In comparison, the proposed equations show high accuracy and low variation.

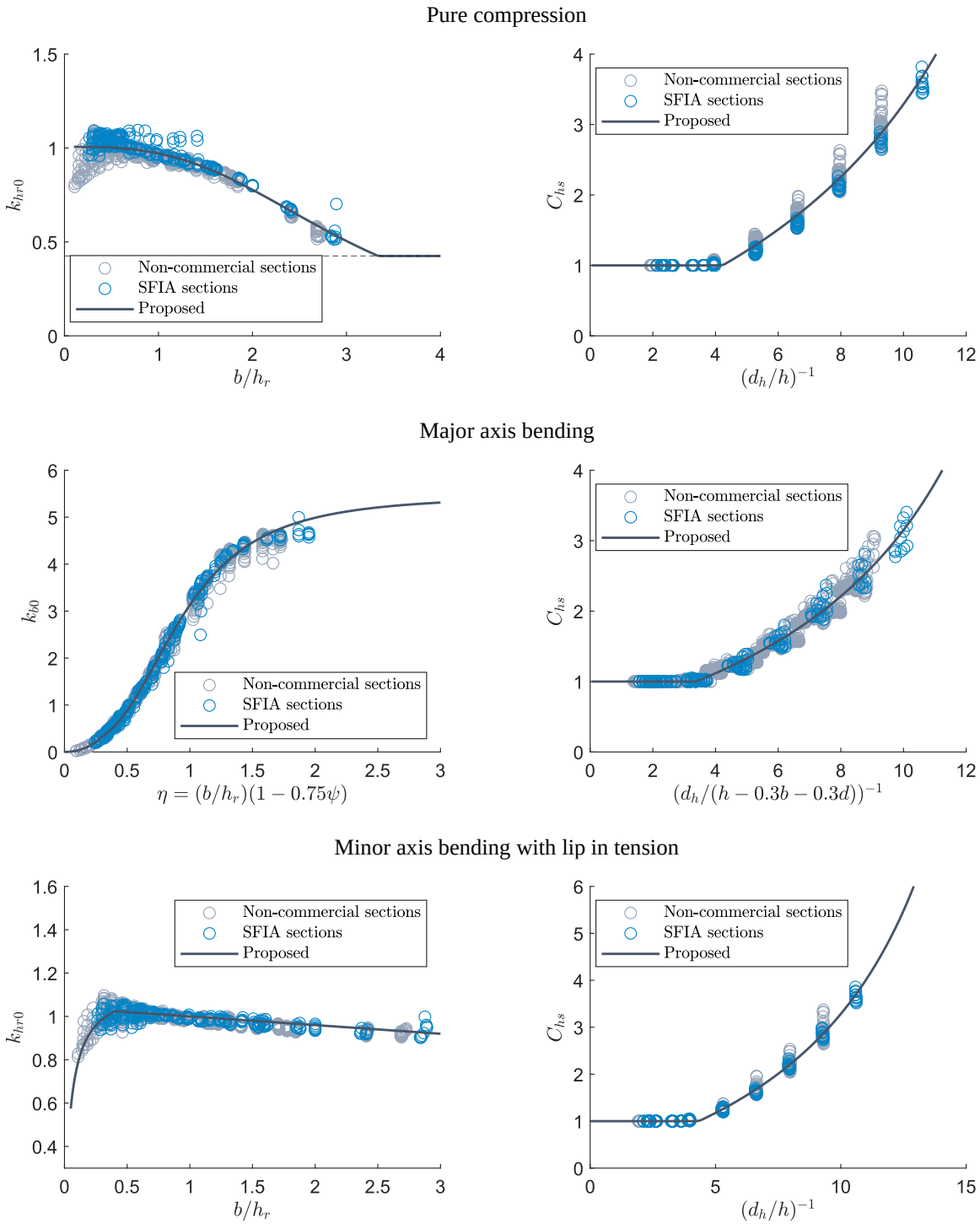

Figure 6: Proposed equations for sections with centered web holes compared to finite strip analysis data

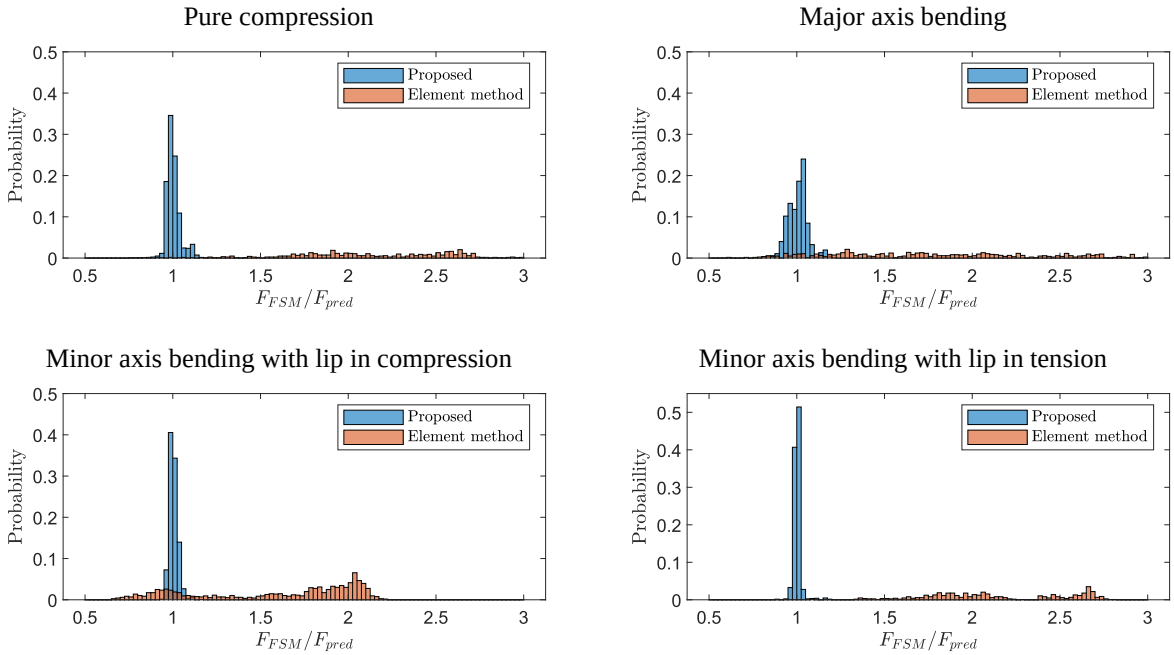

Figure 7: Histogram of the accuracy of the proposed equations for sections with centered web holes

Table 2: Statistical summary of proposed equations for sections with centered web holes

	SFIA (n=244)		Non-commercial (n=984)	
Loading case	Mean	COV	Mean	COV
Pure compression	1.00	0.04	1.00	0.04
Major axis bending	0.99	0.06	1.01	0.05
Minor axis bending with lip in compression	1.01	0.03	1.00	0.02
Minor axis bending with lip in tension	1.00	0.01	1.00	0.02

5.3 Application to non-standard hole lengths

Although this study prioritizes maximizing accuracy for standard hole lengths, the proposed equations can be modified to apply to members with non-standard hole lengths. For non-standard hole lengths, the non-standard hole length modification factor C_h is used in lieu of C_{hs} in the proposed equations. The value of C_h can be approximately determined using C_{hs} as expressed in Eq. 35 and 36.

When $L_h \leq L_{hs}$

$$C_h = C_{hs} \tag{35}$$

When $L_h > L_{hs}$

$$C_h = \begin{cases} 1 + (C_{hs} - 1)\left(\dfrac{L_{cr\ell,h} - L_h}{L_{cr\ell,h} - L_{hs}}\right)^2 & L_h < L_{cr\ell,h} \\ 1 & L_h \geq L_{cr\ell,h} \end{cases} \tag{36}$$

where L_h is hole length, L_{hs} = 4 in. (102 mm) and $L_{cr\ell,h}$ is the half-wavelength of critical local buckling for a section with a centered web hole

The expression of C_h considers two scenarios. When non-standard hole length is shorter than or equal to the standard hole ($L_h \leq L_{hs}$), C_h can be conservatively set to be equal to C_{hs} because a shorter hole length leads to higher critical local buckling stress. When non-standard hole length is longer than the standard hole length ($L_h > L_{hs}$), the value of C_h depends on $L_{cr\ell,h}$, which is the local buckling half wavelength, without considering the limit of hole length. If L_h is greater than $L_{cr\ell,h}$, no modification is needed (C_h = 1), because one full half wavelength of local buckling fits within the hole length. If L_h is not greater than $L_{cr\ell,h}$, parabolic interpolation is used between C_h = 1 and $C_h = C_{hs}$. In Fig. 8, the performance of the C_h equation compared with finite strip analysis data. The proposed C_h equation is found to work well for the cases in Fig. 8.

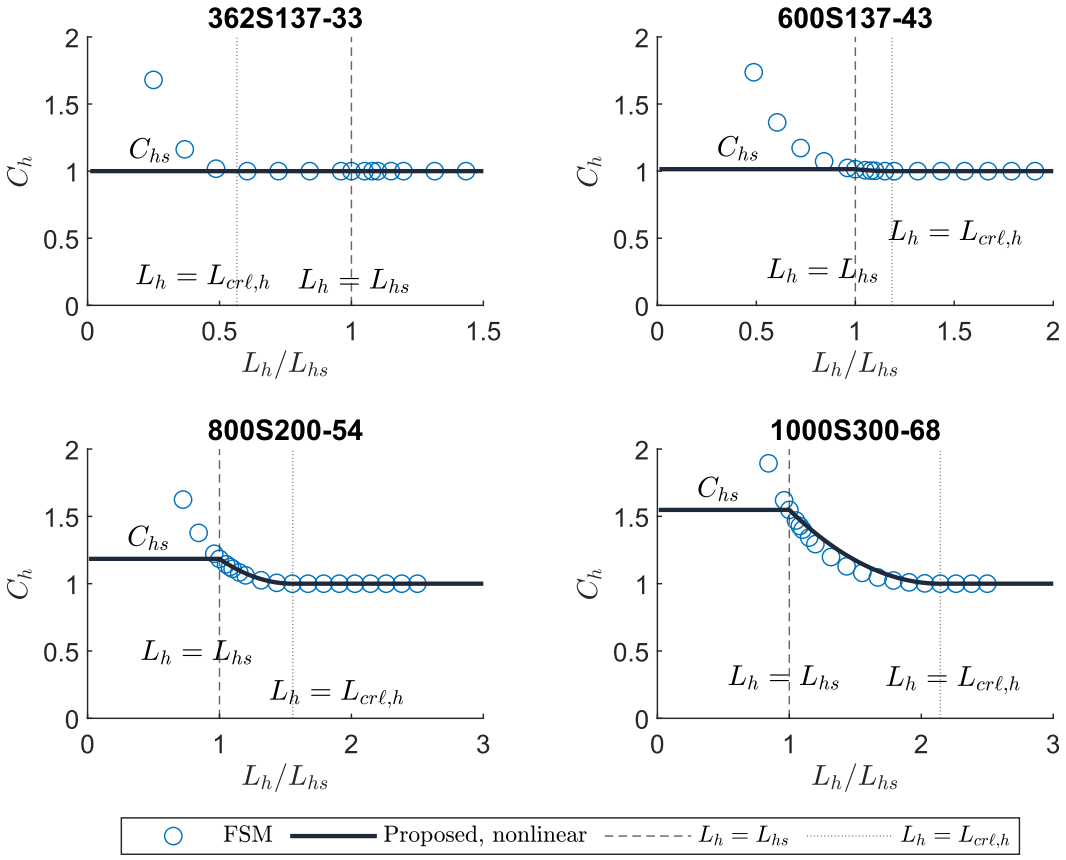

Figure 8: Proposed non-standard hole length modification factor compared to a set of finite strip analysis data

6. Conclusions

This paper presents a new set of analytical equations for determining elastic critical local buckling stresses of lipped channel sections with and without centered web holes. Developed empirically from a large set of finite strip analyses, the proposed equations inherently consider plate interactions and provide explicit considerations of hole dimensions. Compared to the existing AISI analytical equations, the proposed equations come with significant improvements in accuracy and consistency. It is believed that incorporation of the proposed equations into the new editions of the

AISI specification will greatly simplify the process of using DSM in a cold-formed steel structural design workflow.

Acknowledgments

This research is supported by the American Iron and Steel Institute (AISI) and the Steel Framing Industry Association (SFIA) small project/fellowship program. Any opinions, findings, and conclusions or recommendations expressed in this publication are those of the author(s) and do not necessarily reflect the views of the American Iron and Steel Institute and Steel Framing Industry Association

References

Ahdab, M. D., A. W. Fischer, C. Ding, B. Glauz, and B. W. Schafer. 2022. "Local Buckling Expressions for Lipped Channels." *Proceedings of the Annual Stability Conference*. Denver, Colorado.

AISI S100. 2020. *North American Specification for the Design of Cold-Formed Steel Structural Members*. AISI S100-20. Washington, DC: American Iron and Steel Institute.

AISI S240. 2020. *North American Standard for Cold-Formed Steel Structural Framing*. AISI S240-20. Washington, DC: American Iron and Steel Institute.

AS/NZS 4600. 2018. *Australian/New Zealand Standard: Cold Formed Steel Structures*.

EN-1993-1-5. 2006. *Eurocode 3. Design of steel structures - Part 1-5: Plated structural elements*. EN-1993-1-5. Brussels, Belgium: European Committee for Standardization.

Gardner, L., A. Fieber, and L. Macorini. 2019. "Formulae for Calculating Elastic Local Buckling Stresses of Full Structural Cross-sections." *Structures*, 17: 2–20. https://doi.org/10.1016/j.istruc.2019.01.012.

Li, Z., and B. W. Schafer. 2010. "Application of the finite strip method in cold-formed steel member design." *Journal of Constructional Steel Research*, 66 (8–9): 971–980. https://doi.org/10.1016/j.jcsr.2010.04.001.

de Miranda Batista, E. 2010. "Effective section method: A general direct method for the design of steel cold-formed members under local–global buckling interaction." *Thin-Walled Structures*, 48 (4): 345–356. https://doi.org/10.1016/j.tws.2009.11.003.

Moen, C. D., and B. W. Schafer. 2009. "Elastic buckling of thin plates with holes in compression or bending." *Thin-Walled Structures*, 47 (12): 1597–1607. https://doi.org/10.1016/j.tws.2009.05.001.

Seif, M., and B. W. Schafer. 2010. "Local buckling of structural steel shapes." *Journal of Constructional Steel Research*, 66 (10): 1232–1247. https://doi.org/10.1016/j.jcsr.2010.03.015.

SFIA. 2018. *Technical guide for cold-formed steel framing products*. Falls Church, VA: Steel Framing Industry Association.

d